Supporting Information

Exploring saccharinate-tetrazoles as selective Cu(II) ligands: structure, magnetic properties and cytotoxicity of copper (II) complexes based on 5-(3-aminosaccharyl)-tetrazoles

A. Ismael,[a,b,c] M.S.C. Henriques,[c] C. Marques,[a] M. Rodrigues,[b] L. Barreira,[a,b] J. A. Paixão,[c] R. Fausto,[b] and M. L. S. Cristiano[a,b]*

[a]Department of Chemistry and Pharmacy, F.C.T., University of Algarve, P-8005-039 Faro, Portugal

[b]Center of Marine Sciences, CCMar, University of Algarve, P-8005-039 Faro, Portugal

[c]CQC, Department of Chemistry, University of Coimbra, P-3004-535 Coimbra, Portugal

[d]CFisUC, Department of Physics, University of Coimbra, P-3004-516 Coimbra, Portugal

*Corresponding author: E-mail: mcristi@ualg.pt

Index:

Details on the determination of metal chelating activities: The metal ion chelating activity was evaluated by spectrophotometry, using selected metal chelating indicators that produce coloured complexes. The chelating activity was determined measuring the colour change that occurs when the indicator goes from its metal ion-bound form to the unbound form. This colour change takes place when the introduced metal chelator removes the metal ion bound to the indicator. For instance, the blue complex of pyrocatechol violet with Cu^{2+} turns yellow (pH 6.0) when copper ions are sequestered by the chelating agent. The change in colour of the solution was measured at 632 nm, and the chelating activity was calculated using the following equation:

$$Chelating\ activity\ (\%) = \left(1 - \frac{absorbance\ of\ sample\ at\ 632\ nm}{absorbance\ of\ control\ at\ 632\ nm}\right) \times 100$$

The complex formed between PV and Cu^{2+} absorbs at 632 nm, whereas PV dissociated from the metal results in a considerable decrease of the absorption at 632 nm. A solution containing the complex PV and Cu^{2+} was used as a control, and introduced in the equation "absorbance of control at 632 nm" to normalize the absorbance in the range [0-1]. Addition of chelating agent (EDTA, TS or 2MTS) to the mixture of PV and Cu^{2+} resulted in a reduction of absorption at 632 nm, expressed in the equation as "absorbance of sample at 632 nm". It should be noticed that these changes in absorption, result from competition for a coordination position of the studied ligand and the PV molecule, promoting release of PV, so that the introduced ligand can be coordinated with Cu^{2+} to form the new complex. Therefore, the amount of PV released is responsible for the change in absorbance. The chelating activity of the ligand under study is the difference between 1 (when all the PV molecules are released) and the normalized absorbance of the PV molecules remaining coordinated with Cu^{2+}.
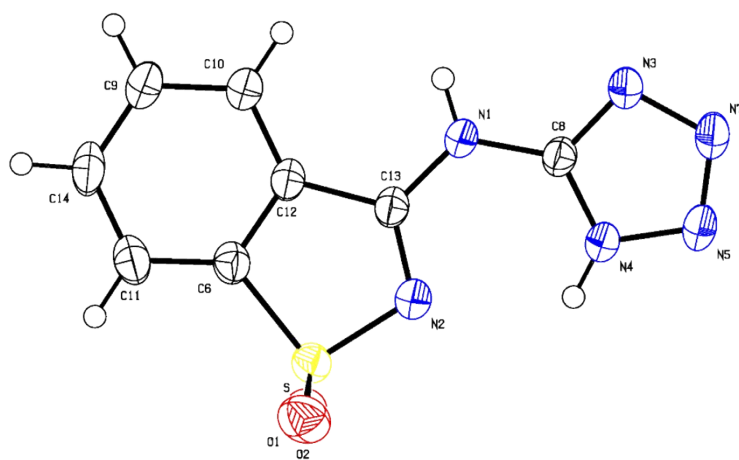
Figure S1. ORTEPII plot of the **TS** (from single crystal XRD data). Displacement ellipsoids are drawn at the 50% probability level.
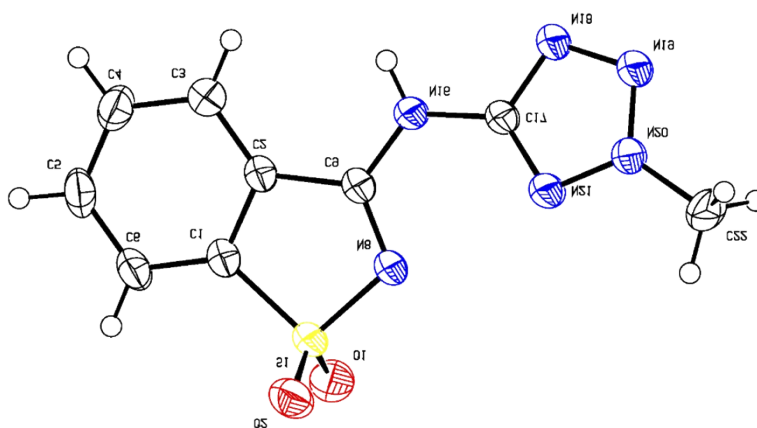

Figure S2. ORTEPII plot of the **2MTS** (from single crystal XRD data). Displacement ellipsoids are drawn at the 50% probability level.
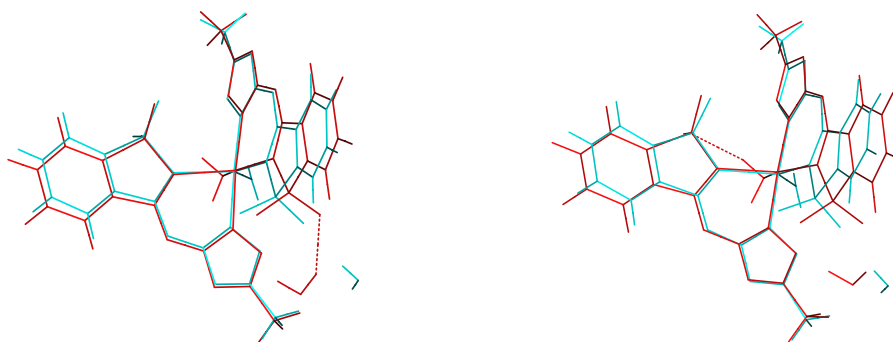
Figure S3. Optimized geometry of the complex **2** *vs.* observed structure in the crystal. The drawing in blue is the starting geometry extracted from the XRD data and the drawing in red shows the optimized structure obtained from the quantum-chemistry calculations. *Left*: ROHF; *Right*: DFT/UB3LYP.
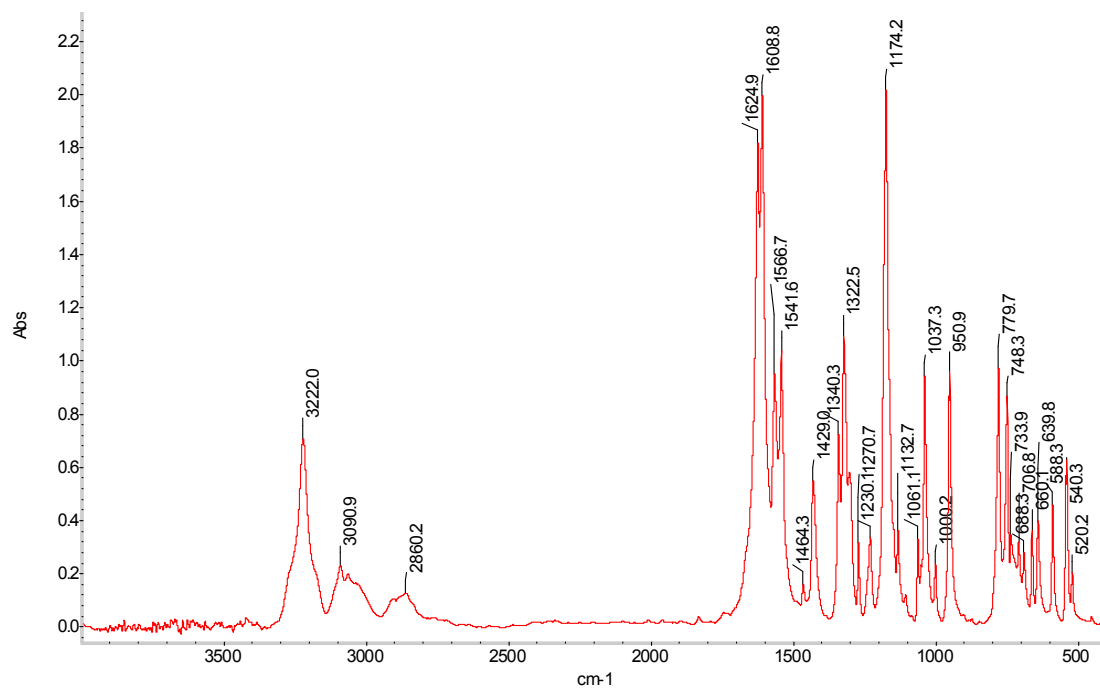

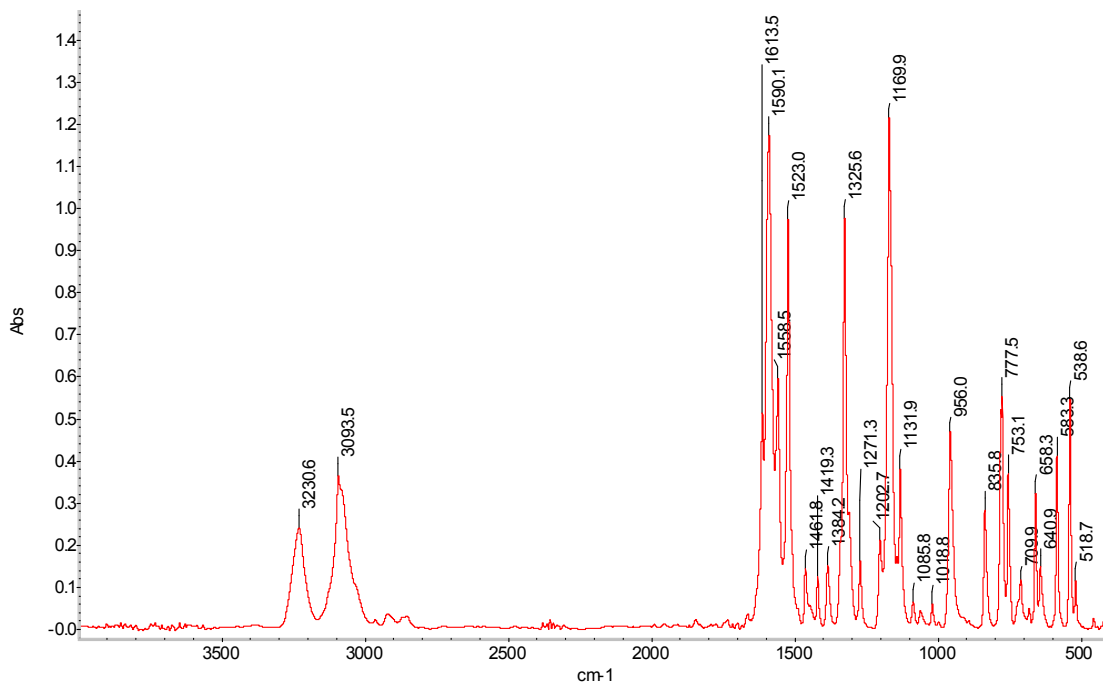**Figure S4**. Infrared spectrum of **TS** (KBr pellet; room temperature).

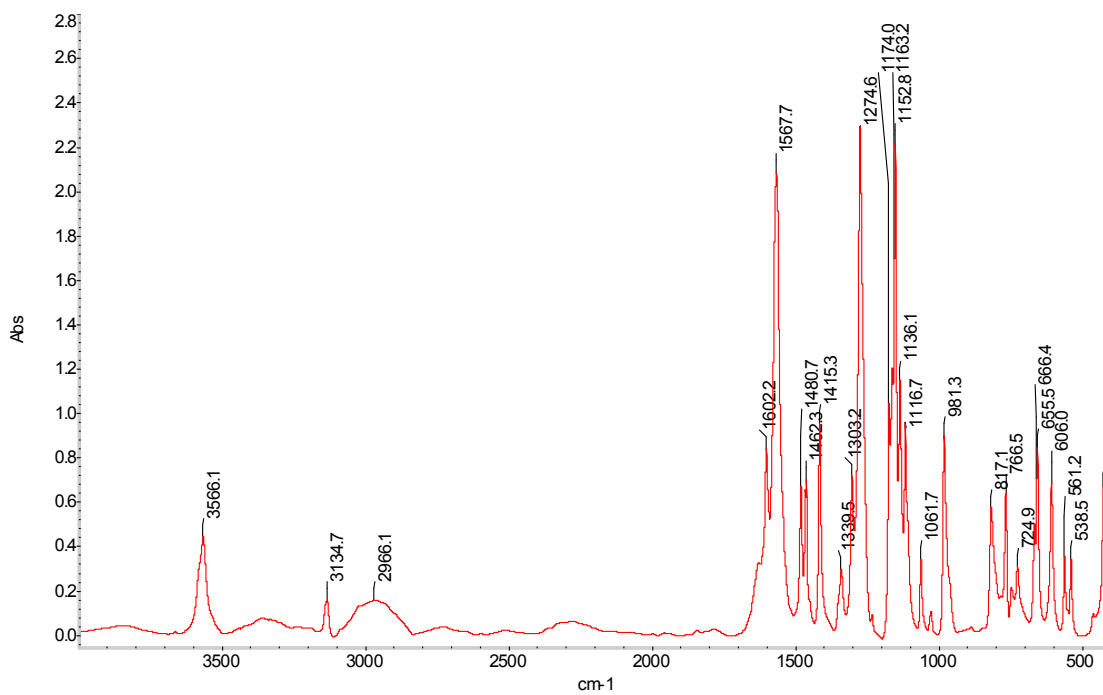**Figure S5**. Infrared spectrum of **2MTS** (KBr pellet; room temperature).

Figure S6. Infrared spectrum of complex **1** (KBr pellet; room temperature).
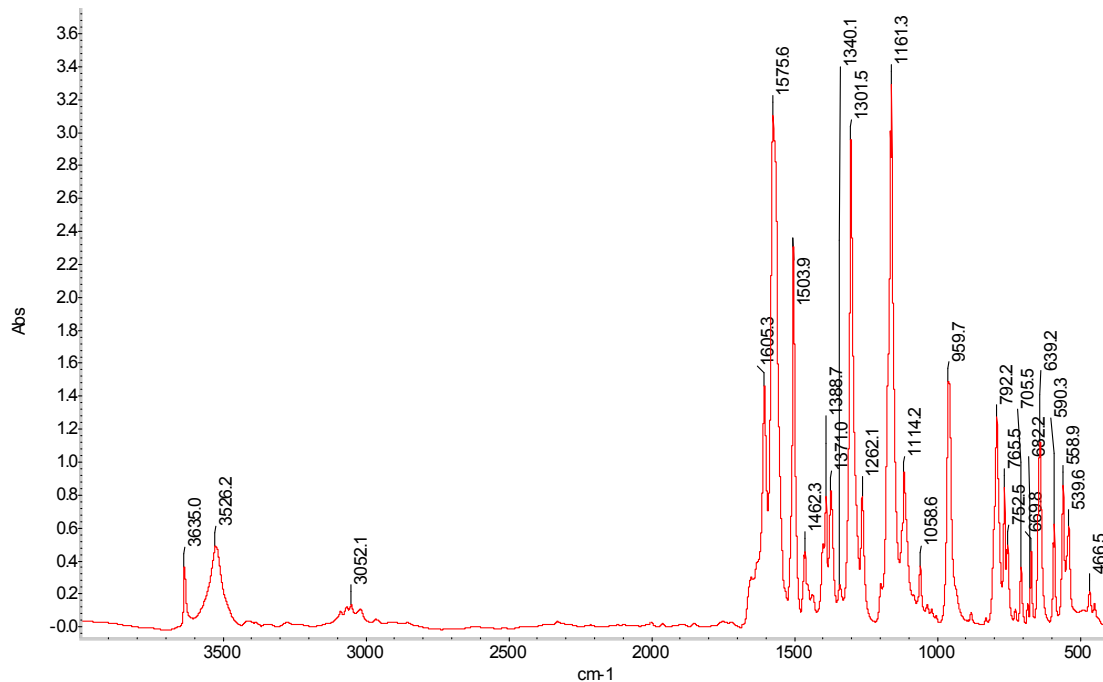
5

Figure S7. Infrared spectra of complex **2** (KBr pellet; room temperature).
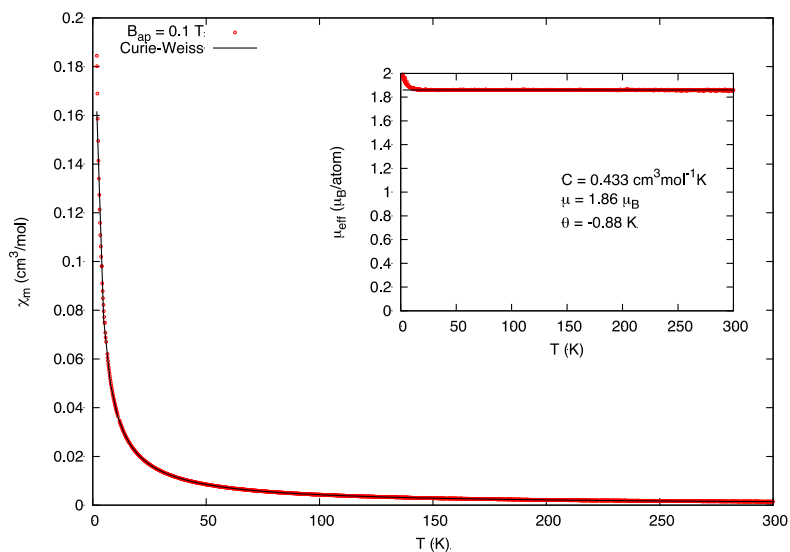
Figure S8. Molar magnetic susceptibility of complex **1** as function of temperature measured with an applied magnetic field of 0.1 T. The line corresponds to the least-squares fit of the data to a modified Curie-Weiss law, $\chi_m = C/(T - \theta) + \chi_0$. The insert depicts the effective moment, $\mu_{eff} = \sqrt{8(\chi_m - \chi_0)(T - \theta)/n}$, where $n = 1$ is the number of magnetic ions per formula unit and θ and χ_0 are given from the fit .

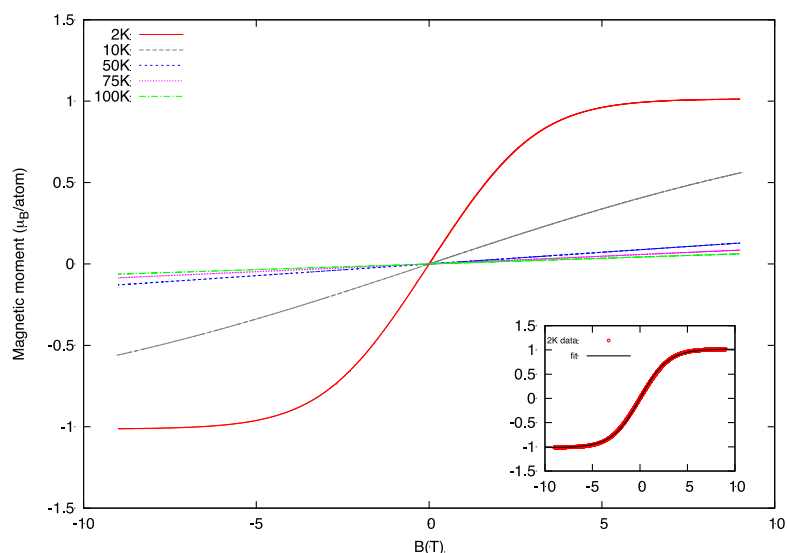**Figure S9**. Magnetization as function of field, expressed as magnetic moment per Cu^{2+} ion, for complex **1**. The magnetization curves follow closely the paramagnetic Brillouin function (insert: fit to the Brillouin function of the 2 K data). At 2 K the saturated paramagnetic moment at 9 T is 1.02 μ_B/Cu atom.

Table S1. Crystal data and structure refinement of complex **2**, [Cu(2MTS)$_2$(H$_2$O)]·H$_2$O.

Empirical formula	$C_{18}H_{18}CuN_{12}O_6S_2$
Formula weight (g.mol^{-1})	626.09
Temperature (K)	293(2)
Wavelength (Å)	0.71073
Crystal system	Triclinic
Space group	*P-1*
a (Å)	8.4669(3)
b (Å)	11.3079(4)
c (Å)	12.7311(4)
α (º)	97.439(2)
β (º)	98.638(2)
γ (º)	91.496(2)
Volume (Å^3)	1193.65(7)
Z	2
Calculated density (g/cm^3)	1.742
Absorption coefficient (mm^{-1})	1.155
F(000)	638
Crystal size (mm^3)	0.44×0.17×0.11
θ range for data collection (º)	4.548-56.269
Index ranges	-10<*h*<10, -14<*k*<14, -16<*l*<16
Reflections collected/unique	27450/5483 (R_{int} = 0.0278)
Completeness to 2*θ*=27.427º	1.00
Refinement method	Full-matrix least-squares on F^2
Data/restrains/parameters	5483/0/ 366
Goodness-of-fit on F^2	1.028
Final *R* indices [*I* > 2σ(*I*)]	R_1 = 0.0306 wR_2 = 0.0780
R indices (all data)	R_1 = 0.0408 wR_2 = 0.0838
Largest diff. peak and hole	0.425 and -0.451

Table S2. Structural parameters for hydrogen bonds and weaker intermolecular interactions between C-H groups as donors and N and O atoms as acceptors.[a]

	D‑H (Å)	H···A (Å)	D···A (Å)	D‑H···A (º)
O1‑H1A···O2[(i)]	0.85(4)	1.78(4)	2.623(3)	172(4)
O1‑H1B···N16	0.63(4)	2.60(5)	2.948(3)	117(5)
O2‑H2A···N12'[(ii)]	0.84(4)	2.14(4)	2.966(2)	168(3)
O2‑H2B···O10	0.77(4)	2.11(4)	2.886(2)	176(4)
C8‑H8···N14'[(ii)]	0.93	2.61	3.499(3)	160.8
C18'‑H18D···O10[(i)]	0.96	2.57	3.377(3)	141.5
C18'‑H18E···N12[(iii)]	0.96	2.65	3.517(3)	150.9
C18'‑H18F···O11[(ii)]	0.96	2.64	3.529(3)	154.1

[a] Symmetry codes: (i) 1-x,-y,1-z; (ii) –x,-y,1-z; (iii) x,-1+y,z.